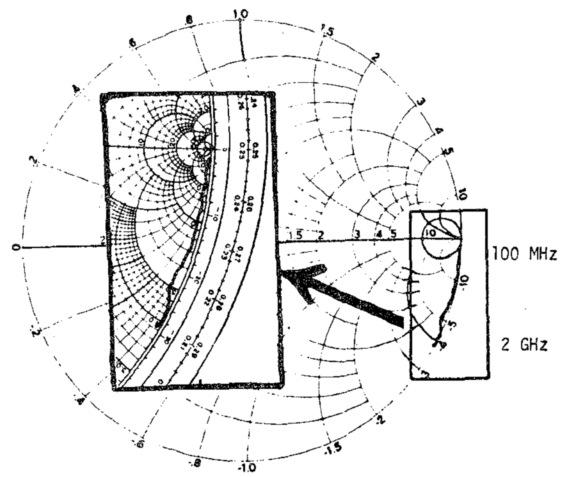

Fig. 2. Varactor reflection coefficient at *O V* bias.

capacitance. The device-chip impedance was calculated from the reflection coefficient measurements using this model.

The calculated varactor capacitance was frequency independent and within experimental error had the same value as measured at 1 MHz. The calculated series resistance is shown in Fig. 1 at bias levels of 0 and -5 V. This shows a similar frequency dependence to previous results ($1/f^2$), asymptotically approaching a small constant value at high frequencies ($\simeq 4\ \Omega$). The possibility of small measurement errors producing large uncertainties in the calculated resistance has been pointed out by Uhlir [6] and a simple consideration of the effects of measurement error produces a plausible explanation for the observed frequency dependence.

Having calibrated the network analyzer in the standard manner, using a short-circuit and a shielded open-circuit with known stray capacitance, the diode's reflection coefficient was measured. The phase approaches 358° at 100 MHz which is very close to an open-circuit. Fig. 2 shows the diode's reflection coefficient after extracting the package and it can be seen by inspection of the Smith chart that small errors in the reflection coefficient near the open-circuit will produce large errors in the calculated impedance.

Mathematically this sensitivity is expressed by $dZ/d\Gamma$, where

$$Z = Z_0 \cdot \left(\frac{1+\Gamma}{1-\Gamma}\right). \tag{1}$$

Thus

$$\frac{dZ}{d\Gamma} = \frac{2Z_0}{(1-\Gamma)^2} \tag{2}$$

and we note that as $\Gamma \to 1$, $dZ/d\Gamma \to \infty$.

For a capacitor the phase of Γ is proportional to the frequency so from (2) it is apparent that errors in Z will be proportional to $1/f^2$ (given a constant error in $|\Gamma|$). Measurements of the short-circuited line with the varactor removed give a value of approximately 0.99 for $|\Gamma|$, which is most likely to be due to losses at the copper plug. The resistance calculated by putting $|\Gamma| = 0.99$ (representing a maximum error of 1 percent) is plotted in Fig. 1. Note that the measurement accuracy is 1 percent with a repeatability of better than 0.5 percent. This curve fits the measured results better than a "fitted" *RC* circuit and it is significant that the calculated increase in error in reverse bias, due to the lower capacitance of the device and hence a reflection phase nearer to 360°, correlates almost exactly with the measured increase in the apparent series resistance.

Conclusion

Accurate measurements of the small-signal impedance of Schottky barrier diodes have been made in the frequency band 100 MHz–2 GHz. As with previously reported measurements the real part of the impedance shows an inverse-square frequency dependence. However, an investigation into the effects of errors on these measurements (errors which are implicit in the observations of other workers) indicate that any frequency dependence in the device is masked by these errors and so it is not possible to attribute any frequency dependence to the real part of the impedance of Schottky barrier devices in this frequency band.

References

[1] D. E. Sawyer, "Surface dependent losses in variable reactance diodes," *J. Appl. Phys.*, vol. 30, p. 1689, Nov. 1959.
[2] S. T. Eng and R. Solomon, "Frequency dependence of the equivalent series resistance for a germanium parametric amplifier diode," *Proc. IRE*, vol. 50, p. 358, Mar. 1960.
[3] S. T. Eng, "Characterisation of microwave variable capacitance diodes," *IRE Trans. Microwave Theory Tech.*, vol. MTT-9, p. 11, Jan. 1961.
[4] F. J. Hyde *et. al.*, "Varactor diode measurements," *Radio Electron. Eng.*, vol. 31, p. 67, Feb. 1966.
[5] C. Toker and F. J. Hyde, "The series resistance of varactor diodes," *Radio Electron. Eng.*, vol. 32, p. 165, Sept. 1966.
[6] A. Uhlir, "Apparent frequency dependence of the series resistance of varactor diodes," *Proc. IEEE*, vol. 51, p. 1246, Sept. 1963.
[7] R. G. Ranson, "The design of transferred electron amplifiers," Ph.D. thesis, Leeds Univ., Leeds, England, 1979.
[8] J. McBretney and M. J. Howes, "Electrical characterization of transferred electron devices by a novel galvanometric technique," *IEEE Trans. Microwave Theory Tech.*, vol. 27 p. 256, Mar. 1979.

Transmission Loss of the Double-Strip Modified *H* Guide at 50 GHz

MITSUO KAWAMURA, MEMBER, IEEE, AND YOSHIHIRO KOKUBO

***Abstract*—A double-strip modified *H* guide has been theoretically and experimentally investigated at 50 GHz. The potential applications of this guide as a low-loss transmission line are discussed.**

I. Introduction

Double-strip modified *H* guide (DS*H* guide) has often been reported, [1]–[5] but very few papers have discussed its transmission characteristics in the millimeter waves region. DS*H* guide has in general less transmission loss than the single strip *H* guide does. This paper describes the experimentally and theoretically investigated results of a DS*H* guide at millimeter wavelength.

II. Theory

The DS*H* guide in consideration is composed of two parallel conducting plates and two parallel dielectric slabs, placed perpendicularly to the plates, as shown in Fig. 1, where b refers to the separation between the two plates, *de* the thickness of the

Manuscript received July 20, 1979; revised November 7, 1979.
The authors are with Tokyo Institute of Technology, Department of Physical Electronics, Tokyo, Japan.

0018-9480/80/0400-0430$00.75 ©1980 IEEE

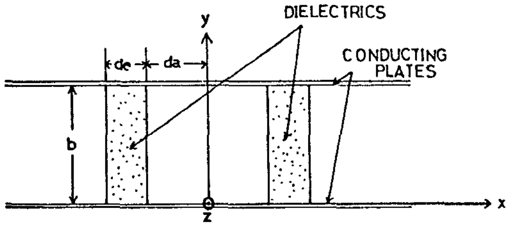

Fig. 1. Cross section of a double strip modified H guide.

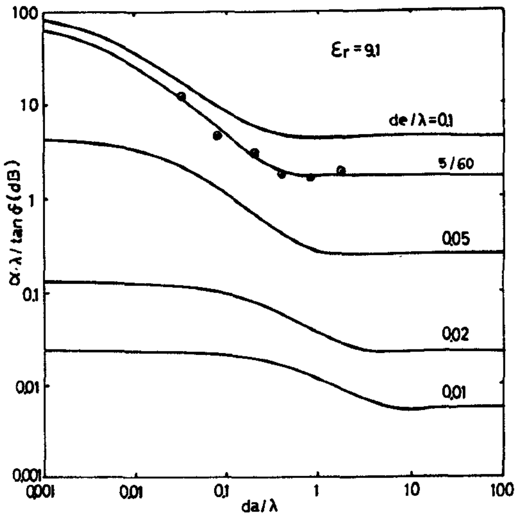

Fig. 2. Calculated transmission loss of a DSH as a function of the separation between two dielectric slabs and its comparison with the experimental data.

dielectric slabs, and da the half of separation between the two dielectric slabs. Rectangular coordinates are used as shown in Fig. 1. It is assumed that the propagation mode in this guide is the TMS symmetrical or PM_{11}^{0} mode, [4] the fundamental mode, and that the direction of propagation is toward the Z axis.

The following four equations determining propagation constant are derived:

$$k_x^2 + k_y^2 + k_z^2 = \epsilon_r k_0^2 \tag{1}$$

$$-\alpha_x^2 + k_y^2 + k_z^2 = k_0^2 \tag{2}$$

$$k_y = \pi / b \tag{3}$$

$$\tan k_x de = \frac{k_x \alpha_x \epsilon_r (1 + \tanh \alpha_x da)}{k_x^2 - \alpha_x^2 \epsilon_r^2 \tanh \alpha_x da} \tag{4}$$

where

(k_x, k_y, k_z)	x,y,z components of propagation constant in each dielectric slab,
(α_x, k_y, k_z)	x,y,z components of propagation constant in the region outside dielectric slab,
ϵ_0	free space dielectric constant,
ϵ_r	relative dielectric constant of the dielectrics,
k_0	$\omega\sqrt{\epsilon_0 \mu_0}$,
ω	angular frequency.

Equation (4) is the characteristic equation for this system.

Attenuation of this guide is mainly caused by dielectric loss (characterized by attenuation constant α_D) and conductor loss (attenuation constant α_M). Equations defining α_D and α_M have been derived and are shown below:

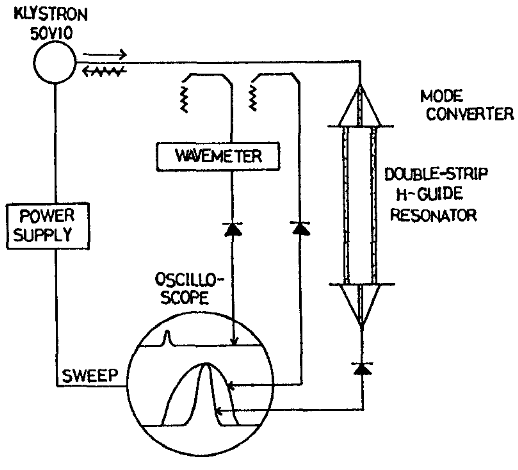

Fig. 3. Test configuration.

$$\alpha_D = \frac{\frac{\tan\delta}{2\epsilon_r}\left\{(k_y^2 + k_z^2)B_+ + k_x^2 B_-\right\}}{k_z(A + B_+/\epsilon_r + 1/2\alpha_x)} \tag{5}$$

$$\alpha_M = \frac{\frac{2\omega\epsilon_0}{\delta_c \sigma b}\frac{k_y^2}{k_y^2 + k_z^2}(A + B_+ + 1/2\alpha_x)}{k_z(A + B_+/\epsilon_r + 1/2\alpha_x)} \tag{6}$$

where

$\tan\delta$	dielectric loss tangent of the dielectric slab,
δ_c	skin depth of the conductor,
σ	conductivity of the conductor.

Further A and $B_\pm$ are given by

$$A = \left(\frac{k_x \cos k_x de + \alpha_x \epsilon_r \sin k_x de}{k_x \cosh \alpha_x da}\right)^2 \cdot \left(\frac{\sinh 2\alpha_x da}{4\alpha_x} + \frac{da}{2}\right) \tag{7}$$

$$B_\pm = \frac{1}{2}\left(1 + \frac{\alpha_x^2 \epsilon_r^2}{k_x^2}\right)de \pm \frac{1}{4k_x}\left(1 - \frac{\alpha_x^2\epsilon_r^2}{k_x^2}\right)\sin 2k_x de \pm \frac{\alpha_x \epsilon_r}{2k_x^2}(1 - \cos 2k_x de). \tag{8}$$

Solid lines of Fig. 2 show the overall theoretical attenuation in the DSH guide as a function of da normalized to λ with de normalized to λ as a parameter. From this figure the DSH guide features less transmission loss than a comparable single strip H guide. The difference depends on the parameter de/λ. Equations (5) and (6) are in agreement with the corresponding formulas given in [4].

III. Experiments

The transmission loss of a DSH guide was measured at 50 GHz using a resonance method. The test configuration is shown in Fig. 3. The input power fed by a klystron 50V10 is coupled to the DSH guide resonator through a mode converter as shown in Fig. 4. TE_{10} mode generated from the klystron is transformed into the single strip H guide mode, which in turn successively excites the DSH guide into the desired mode. The dimension of the horn transition, the diameter and the number of coupling holes in the part of the mode converter are as shown in the figure. The insertion loss of the mode launcher is 1.0–1.5 dB. In this configuration, the quality factor Q of the resonator is

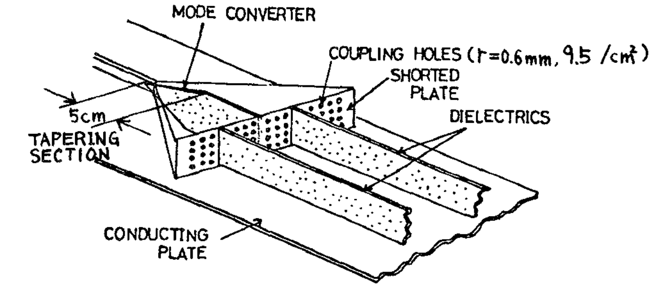

Fig. 4. External appearance of the mode converter in use with an upper conducting plate removed.

given by

$$\frac{1}{Q}=\frac{2k_z(A+B_+/\epsilon_r+1/2\alpha_x)}{k_0^2(A+B_++1/2\alpha_x)}\alpha+\frac{C}{l} \tag{9}$$

where C is a constant which is determined from the ohmic loss due to the devices such as the shorted plates and coupling holes except the DS*H* itself, and l is the length of the DS*H* guide. Therefore, the attenuation constant α is determined when the Q of this system is measured at the several different lengths of the DS*H* guide. In our experiment five different lengths were properly chosen between 0.2 m and 1.0 m.

The material chosen for the dielectric slabs was alumina. The thickness of the slabs was fixed at 0.5 mm throughout the experiments. ϵ_r and $\tan\delta$ of the slabs were found 9.1 and 1.0×10^{-3}, respectively, by the measurement at 50 GHz. Two conducting plates are copper. The space between the two plates was filled with styrofoam to support the dielectric sheets and maintaining proper position. ϵ_r and $\tan\delta$ of this material were found 1.02 and 8×10^{-5} by the measurement at 50 GHz. b is 3 cm.

The experimental results concerning attenuation versus da are shown in Fig. 2. Circled marks represent measured points and solid line denotes theoretical prediction with the $\tan\delta$ of 1.5×10^{-3}. In this graph the loss tangent used for the theoretical curve has been a little bit differently chosen in such a way that the best fit for the measured points was achieved. However, fairly good agreement of the tendency between the theoretical and experimental data has been achieved.

IV. Conclusion

The DS*H* guide was theoretically and experimentally investigated at 50 GHz and the experimental results were satisfactorily explained by the theoretical predictions. The transmission loss of the DS*H* guide has advantages of less than that of single-strip *H* guide under the condition of constant cross-sectional area of dielectrics. The difference of 4.5 dB/m was obtained by our experimental waveguide dimensions and material.

References

[1] A. Doswell and D. J. Harris, "Modified *H* guide for millimeter and submillimeter wavelengths," *IEEE Trans. Microwave Theory Tech.*, vol. MTT-21, pp. 587–589, Sept. 1973.

[2] R. J. Batt and H. L. Bradley, A. Doswell, and D. J. Harris, "Low-mode low-loss waveguides and open-resonator techniques at submillimeter wavelengths," in 1974 *Int. Conf. Submillimeter Wave and Their Applications, Conf. Dig.*, (Atlanta, GA), pp. 30.

[3] R. J. Batt, H. L. Bradley, A. Doswell and D. J. Harris, "Waveguide and open-resonator techniques for submillimeter waves," *IEEE Trans. Microwave Theory Tech.*, vol. MTT-22, pp. 1089–1094, Dec. 1974.

[4] R. F. B. Conlon and F. A. Benson, "Propagation and attenuation in the double-strip *H* guide," *Proc. Inst. Elect. Eng.*, vol. 113, pp. 1311–1320, Aug. 1966.

[5] F. J. Tischer, "*H* Guide with laminated dielectric slab," *IEEE Trans. Microwave Theory Tech.*, vol. MTT-18, pp. 9–15, Jan. 1970.

Letters

A Simple Full-Band Matched 180° *E* Plane Waveguide Bend

FRANS C. DE RONDE

A recent publication by Kashyap [1] describes a simple 180° waveguide bend. However, a similar structure of marginally increased complexity has been used in the past to make a matched bend over a whole waveguide band [2].

In order to try to reduce the size of a long straight plain waveguide in use for a Reflectoscope [3], serpentine bends, especially in the *E* plane in order to have minimum reflection, were considered.

The 180° constant radius bends are easily made by using two sections of standard waveguide, soldered one on top of the other with a concave constant radius plunger forming the actual bend (Fig. 1). In this way the separation between the guides was just equal to double the wall thickness, namely 0.1 in for standard *X*-band waveguide (WR 90). The concave movable short was constructed from a square piece of brass, machined with close tolerances to assure good contact with the broad faces of the waveguide walls.

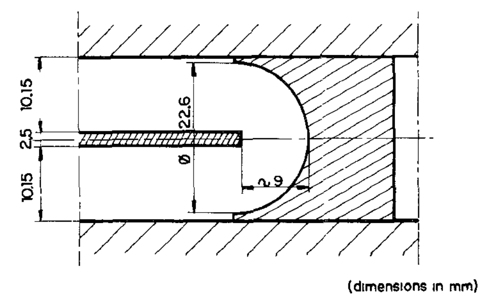

Fig. 1 Unmatched constant radius *E* bend.

The shunt capacitance, formed by the discontinuity between straight and curved waveguides, gave a maximum reflection of about 5 percent, occurring at the highest frequency in the band (8.2–12.4 GHz). Complete cancellation of this reflection was

Manuscript received July 16, 1979; revised November 11, 1979.
The author is with LEP, BP 15-94450 Limeil-Brévannes, France.

0018-9480/80/0400-0432$00.75 ©1980 IEEE